Pharmaceutical Nanotechnology, 2016, *4*, 3-15

IT-143, A Polymer Micelle Nanoparticle, Widens Therapeutic Window of Daunorubicin

Tara Lee Costich, Adam Carie, J. Edward Semple, Brad Sullivan*, Tomas Vojkovsky, Tyler Ellis, Taylor Buley, Suzanne Bakewell* and Kevin Sill

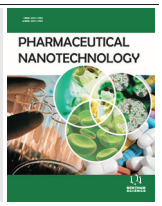

Intezyne Technologies, Tampa, FL, USA

T.L. Costich

Abstract: ***Background***: Daunorubicin is an anthracycline family chemotherapeutic indicated for the treatment of acute myelogenous and acute lymphoblastic leukemia. Daunorubicin has a narrow therapeutic window.

Objective: To extend circulation time, decrease toxicity and improve the efficacy of daunorubicin, we encapsulated the drug in our nanoparticle drug delivery platform.

Method: IT-143 is a lyophilized formulation of daunorubicin, non-covalently encapsulated in the hydrophobic core of a polymer micelle. Hydroxamic acid-containing triblock polymers (ITP-102) support ferric crosslinking between the polymer chains, increasing stability for improved drug circulation and allowing a tumor targeted pH dependent release of the encapsulated daunorubicin.

Results: Formulation characterization demonstrates a 3.7% weight loading (w/w) of daunorubicin and an average particle diameter of 58 nm. IT-143 has an *in vitro* cytotoxicity of 60-100 nM, comparable to free drug cytotoxicity of 67-114 nM. We compared daunorubicin pharmacokinetics between free drug and IT-143 *in vivo* and the maximum serum concentration of daunorubicin from IT-143 was increased 50-fold. At equivalent doses IT-143 eliminated *in vivo* gross toxicity observed at daunorubicin's maximum tolerated dose of 7.5 mg/kg, and increased the equitoxic dose to 17.5 mg/kg. Furthermore, IT-143 improved anti-tumor efficacy. Studies in 3 xenograft models (HCT116, HT-1080 and MNNG-HOS) compared intravenous bolus administration of IT-143 at equivalent and equitoxic doses to daunorubicin treatment. IT-143 increased the inhibition of tumor volume growth in all models.

Conclusion: These studies indicate that the encapsulation of daunorubicin by IT-143 widens the therapeutic window of daunorubicin treatment with reduced toxicity and increased antitumor efficacy.

Keywords: Anthracyclines, hydroxamic acid, *in vivo* efficacy, pharmacokinetics, polymer micelle, therapeutic window.

1. INTRODUCTION

Anthracyclines have been investigated as conventional chemotherapeutics for over 50 years. Their antitumor potency is paired with chronic cardiac toxicities and myelosuppression [1-4]. Daunorubicin (or daunomycin) is a DNA intercalating agent that affects the action of topoisomerase II, thus impeding replication and the production of macromolecules [5]. This initiates the DNA damage checkpoint pathway and inhibits cell growth. Daunorubicin also causes severe local tissue necrosis from injection extravasation and is administered in a rapid intravenous infusion [6]. Dosing is further hindered by low solubility and drug hydrophobicity [7]. Other physiological barriers daunorubicin faces as a small molecule include stereochemistry that supports π -stacking, making it highly reactive and highly toxic. Daunorubicin's activity is influenced by its aglycone moiety and glycosidic linkage generating affinity for hydrolysis, oxidation, and cleavage reactions.

*Address correspondence to these authors at the Intezyne Technologies, Tampa, FL, USA; Tel/Fax: +1-813-910-2120; E-mails: suzanne.bakewell@intezyne.com; and brad.sullivan@intezyne.com

2211-7393/16 $58.00+.00

These small molecule characteristics allow it to infiltrate all tissue types without tumor selectivity, causing systemic toxicities. These traits also account for decreased plasma circulation due to renal clearance, and protein opsonization via the mononuclear phagocyte system (MPS), thereby requiring higher frequency dosing to achieve tumor exposure effectiveness.

The limitations of anthracyclines make them ideal candidates for drug delivery technologies. Formulation strategies have included encapsulation in PEGylated liposomes, polymeric micelles, polymer conjugates, peptide conjugates, gold and silica nanoparticles, carbon nanotubes, and cyclodextrin nanoparticles [8]. Doxil, a PEGylated liposomal formulation of doxorubicin, was approved by the FDA for clinical use in 1995 for Karposi's sarcoma, and later for ovarian cancer and multiple myeloma [9]. The Doxil formulation allows doxorubicin to circulate for prolonged periods of time resulting in slow release of the drug and allows for accumulation of liposomes in the tumor environment [10]. Doxil demonstrated reduced cardiotoxicity while demonstrating equivalent antitumor efficacy in a phase III clinical trial in metastatic breast cancer [11, 12].

Biodegradable polymeric nanoparticle drug carriers hold potential to provide an escape from the biological barriers that daunorubicin faces. Nanoparticles developed to overcome delivery obstacles ideally should do so without chemical alteration or degradation of the active drug. Solid nanoparticles and chemical drug conjugates to nanoparticle moieties are dependent on particle cleavage that decreases bioavailability or drug functionality [13]. At the same time, nanoparticle delivery should allow for adequate shielding and active drug release that has been attempted in micelles by crosslinking [14]. Polymer or liposomal self-assembly without crosslinking results in reduced stability in circulation and premature drug release [14]. Peripheral micelle crosslinking may not provide sufficient stability or alternatively, results in too much shielding and insufficient drug release. Furthermore, micelle crosslinking cannot interfere directly with the drug. Therefore, key requirements of drug delivery include transportation with protection from reactive blood conjugates and the ability to dissociate and release the drug in the targeted tissue with optimal timely release.

The tumor microenvironment provides the unique pathophysiology for nanoparticle delivery. A tumor's need for metabolic nutrients from the constant cancer cell proliferation demands angiogenesis for survival. This vasculature development is initiated so rapidly by the vascular growth factors that it has inherit defects: gaps between endothelial cells that increases permeability, anomalous architecture such as excessive vascular density, unmanaged branching, and exaggerated lengthening coupled with the retention of lymphatic macromolecules from inadequate clearance [15-17]. The combination of these peculiarities is termed the Enhanced Permeability and Retention (EPR) effect [17-19]. These characteristics create a tumor microenvironment that is ideal for shielded chemotherapeutic drug delivery [20-23]. The constituted lymphatic drainage of normal tissue surrounding the tumor tissue may increase clearance away from normal tissue allowing for more tumor exposure and reduced side effects.

Intezyne's goal is to further widen the therapeutic window for anthracyclines by encapsulating daunorubicin in a stabilized polymer micelle. The formulation was designed to not only prolong circulation, but also to actively deliver daunorubicin to the tumor and tumor microenvironment based on a pH-dependent release of the drug. In doing so, our formulation provides a safer, more effective means for drug delivery without the need for chemical conjugation or enzymatic activation.

2. MATERIALS AND METHODS

2.1. Synthesis of Polymer ITP-102

ITP-102, PEG_{12K}-NH-b-p-[L-Glu$(NHOH)_5$-co-D-Glu$(NHOH)_5$]-b-p-[D-Phe_{15}-co-L-Tyr_{25}]-Ac, a novel hydroxamic acid triblock polymer (HATB) with mixed, nonracemic D- and L-amino acid stereochemistry in the crosslinking and core blocks that features a metal-chelating polyglutamic hydroxamate crosslinking moiety was synthesized in two steps as summarized below. For starting materials, we used mPEG_{12K}-NH_2 as the free base (PDI=1.01-1.03, overall yield > 95%) and highly purified *N*-carboxyanhydrides (NCAs). The latter were prepared from dried α-amino acids by reaction with phosgene or diphosgene in anhydrous THF at 50-55°C followed by filtration through Celite and two precipitations from THF, heptane mixtures (NCA yields generally 85-97%

on ≥ 0.5 mole scale). Our synthetic route is summarized in Scheme **1**.

The key protected triblock intermediate $mPEG_{12K}$-NH-b-p-[L-Glu(OBn)$_5$-co-D-Glu(OBn)$_5$]-b-p-[D-Phe$_{15}$-co-L-Tyr (OAc)$_{25}$]-Ac (**1**) was assembled in a one-pot operation by ring-opening polymerization of the appropriate *N*-carboxyanhydride (NCA) monomers using $mPEG_{12K}$-NH_2 as the macroinitiator. Thus, vacuum-dried $mPEG_{12K}$-NH_2 was dissolved in a mixture of anhydrous dichloromethane, *N,N*-dimethylacetamide (2:1, v/v), treated with L-Glu(OBn) NCA (5 eq.) and D-Glu(OBn) NCA (5 eq.), and the reaction mixture was allowed to stir at room temperature. After 22 hours, GPC analysis (DMF, 0.1% LiBr) indicated complete consumption of the Glu(OBn) NCAs and clean formation of the corresponding diblock intermediate, $mPEG_{12K}$-NH-b-p-[L-Glu(OBn)$_5$-co-D-Glu(OBn)$_5$]-NH_2. Then, D-Phe NCA (15 eq.) and L-Tyr (OAc) NCA (25 eq.) were added. The solution was stirred at ambient temperature for two hours (copious CO_2 evolution) and then heated to 35°C for 32 hours, at which point the reaction was deemed complete by GPC. The resultant terminal amino intermediate was acetylated (Ac_2O, 10 eq., NMM, 11 eq., DMAP, 1 eq.) and stirring was continued for seven hours. Dichloromethane was removed *in vacuo*, the residue was precipitated with isopropanol (IPA), filtered, then further purified by slurrying in IPA. Standard workup and drying afforded pure intermediate (**1**) in 93.7% yield.

The second step of the synthesis employs a global deprotection-hydroxylamination sequence. Intermediate (**1**) dissolved in THF was treated with hydroxylamine solution (50% aqueous, 5.0 eq./ester moiety) and lithium hydroxide monohydrate (1.0 eq./ester moiety) as catalyst. The reaction was stirred at room temperature for 28 hours, whereupon ^{1}H-NMR analysis (DMSO-d_6) indicated only ~3-4% of unreacted benzyl ester signal remained at δ5.01. The reaction mixture was quenched with acetone (10 eq./NH_2OH) and acetic acid (1 eq./NH_2OH), stirred for 14 hours and then the product was precipitated by addition of excess IPA. Solids were dried overnight *in vacuo* to afford ITP-102 in 97.2% yield as the •3LiOAc complex, as determined by ^{1}H-NMR analysis. Further purification can be effected by slurrying ITP-102 overnight in absolute ethanol with rapid magnetic stirring. Standard workup gave 98.7% recovery of ITP-102 as a fine, colorless, nearly odorless solid. ^{1}H-NMR (DMSO-d_6) analysis indicated the presence of ~2.7% unreacted benzyl ester with no detectable lithium acetate. GPC (CH_3CN: H_2O; 40:60 (v/v), 0.1% TFA; UV, RI, and MALLS detection) provided an Mp of 24,180 daltons for the final polymer.

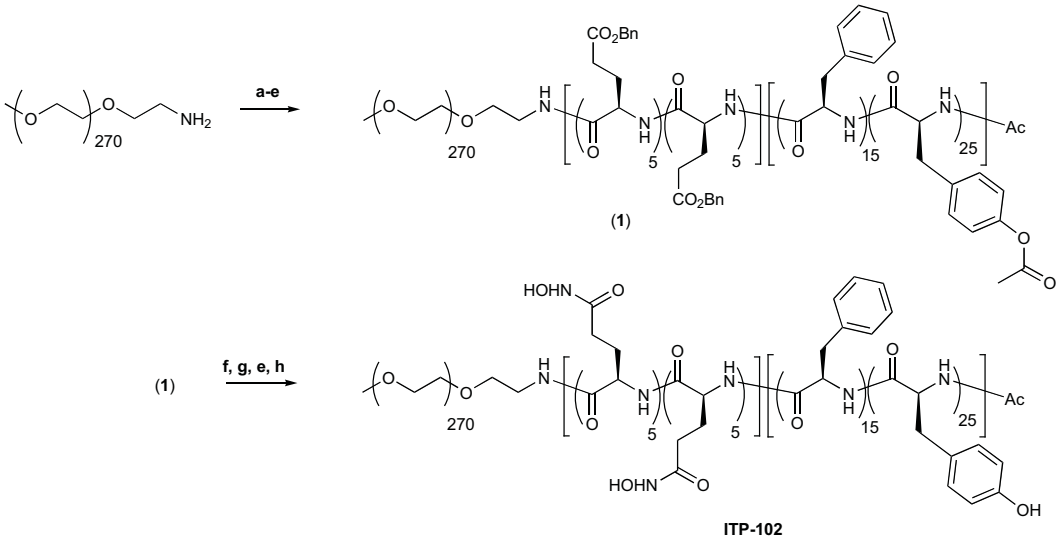

Scheme (1). Reagents and Conditions: (a) Toluene, 50-70˚C, -H_2O; (b) L-Glu(OBn)NCA (5 eq.), D-Glu(OBn)NCA (5 eq.), DCM:DMAC (2:1, v/v), r.t., 22 h; (c) D-Phe NCA (15 eq.), L-Tyr(OAc)NCA (25 eq.), r.t. to 35˚C, 32 h; (d) Ac_2O (10 eq.), NMM (11 eq.), DMAP (1 eq.), r.t., 7 h; (e) IPA precipitations; (f) 50% aq. NH_2OH (5 eq./ester), LiOH•H_2O (1 eq./ester), THF, r.t. 28 h; (g) acetone (10 eq./NH_2OH), AcOH (1 eq./NH_2OH), reflux to r.t., 16 h.; (h) ethanol washing.

2.2. Physiochemical Characterization of IT-143

IT-143 is a lyophilized formulation of daunorubicin encapsulated in a micelle composed of ITP-102 polymer. Daunorubicin was purchased from TEVA, Petach Tikva, Israel (Lot No. 6447AO00414R).

The micelles were formed using an oil in water emulsion formulation technique where the micelles self-assemble as the organic phase evaporates from the aqueous phase. The polymer was dissolved in water at a concentration of 10 mg/mL. The daunorubicin was dissolved in a solution of 20% methanol in dichloromethane (v/v). The feed of daunorubicin for the formulation was 10% of the polymer weight (w/w). Immediately prior to formulation, 0.02% (v/v) triethylamine was added to the organic solvent to convert daunorubicin from the hydrochloride salt to the free base form. The polymer solution was mixed using a high-shear mixer while adding the daunorubicin solution to form an emulsion. This solution was then stirred in a fume hood to allow the organic solvent to evaporate. The formulation was crosslinked by adding iron(III)chloride solution and the pH was adjusted to 7 with NaOH. The formulation was stirred for a minimum of 4 hours, and then concentrated to 20 mg/mL polymer concentration by ultrafiltration using a 10 kD tangential flow filtration filter. Trehalose was added to the formulation as a cryoprotectant/bulking agent, and the formulation was filtered through a 0.2 μm sterile filter and lyophilized.

Weight loading of daunorubicin for IT-143 was determined by HPLC/UV analysis. IT-143 was reconstituted in methanol at a concentration of 2 mg/mL. A standard curve of daunorubicin was prepared in methanol at concentrations of 20, 40, 60, 80, and 100 μg/mL. Daunorubicin content in IT-143 was determined by comparing the peak area for the 2 mg/mL sample of IT-143 to the daunorubicin standard curve.

Average particle diameter and average particle size distribution for IT-143 was determined by dynamic light scattering (DLS) using a Wyatt, Dynapro plate reader. IT-143 was dissolved in 0.9% saline for injection at 1 mg/mL and aliquoted into a 96-well plate in triplicate. Samples were analyzed at 37°C with 10 acquisitions per well and a 30 second acquisition time per sample.

Encapsulation, crosslinking, and pH-dependent release of daunorubicin were determined using a dialysis bag diffusion technique. The reconstituted formulation was dialyzed against phosphate buffer (pH 7.4) for 6 hours and the percentage of daunorubicin in the bag was determined by HPLC/UV analysis.

Encapsulation of daunorubicin was determined by reconstituting IT-143 above the CMC (20 mg/mL) in phosphate buffer (10 mM, pH 7.4). 3 mL of IT-143 solution was then added to a dialysis bag (SpectraPor7, 3500 MWC), placed in a beaker containing 300 mL phosphate buffer (10 mM, pH 7.4), and stirred at low speed for 6 hours. The percentage of daunorubicin remaining in the dialysis bag was determined by comparing the peak areas from the pre and post dialysis samples by HPLC/UV.

Stabilization of the micelle formulation by iron crosslinking was determined by reconstituting IT-143 and uncrosslinked micelle formulation below the CMC (0.2 mg/mL) in phosphate buffer (10 mM, pH 7.4). 3 mL of formulation was added to a dialysis bag (SpectraPor7, 3500 MWC), placed in a beaker containing 300 mL phosphate buffer (10 mM, pH 7.4), and stirred at low speed for 6 hours. The percentage of daunorubicin remaining in the dialysis bag was determined by comparing the peak areas from the pre and post dialysis samples by HPLC/UV.

pH-dependent release of daunorubicin was determined by reconstituting IT-143 below the CMC (0.2 mg/mL) in phosphate buffer (10 mM) at pH 3, 4, 5, 6, 7, 7.4, and 8. 3 mL of each solution was added to a dialysis bag (SpectraPor7, 3500 MWC), placed in a beaker containing 300 mL phosphate buffer (10 mM, pH 7.4), and stirred at low speed for 6 hours. The percentage of daunorubicin remaining in the dialysis bag was determined by comparing the peak areas from the pre and post dialysis samples by HPLC/UV.

2.3. Pharmacokinetics

2.3.1. Pharmacokinetic Sampling in a Cannulated Rat Model

Rats surgically modified with jugular vein catheters were obtained from Envigo. Test articles were reconstituted in 0.9% saline for injection, and 3 rats per group were dosed with either 10 mg/kg

daunorubicin free drug, or 10 and 20 mg/kg daunorubicin equivalent of IT-143 by fast bolus into the jugular vein catheter. 0.2 mL of blood was collected into K2-EDTA tubes at time points of 1 minute, 5 minutes, 15 minutes, 1 hour, 4 hours, 24 hours, and 48 hours post test article administration. Plasma was isolated by centrifugation at 2000 RPM for 5 minutes, aliquoted into 1.5 mL centrifuge tubes, and frozen until processed for HPLC/FLD analysis.

2.3.2. Pharmacokinetic Sampling in a Cannulated Rabbit Model

QTest Laboratories (Columbus, Ohio) was contracted for the rabbit study. Groups were composed of 4 New Zealand White rabbits for daunorubicin free drug at 3 mg/kg, and IT-143 at 1, 3, and 6 mg/kg. Test articles were reconstituted in 0.9% saline and administered by 30-minute infusion via jugular vein catheter. Blood was collected at time points of 1 hour, 4 hours, 8 hours, 24 hours, 48 hours, and 96 hours. Rabbits treated with 3 and 6 mg/kg IT-143 included an additional blood sampling 15 minutes post infusion. Plasma was isolated by centrifugation, frozen, and sent to Intezyne for processing by HPLC/FLD.

2.3.3. Bioanalytical Sample Preparation for HPLC/FLD Analysis

Plasma sampled from cannulated rats and rabbits were prepared for HPLC/FLD analysis using a protein precipitation method with acidified methanol. Plasma was thawed on ice and 50 µL of each sample was added to 150 µL of cold acidified (1% perchloric acid) methanol. Samples were vortexed for 5 minutes and centrifuged at 13,000 RPM for 10 minutes at 4°C. The supernatant was aliquoted into HPLC vials and assayed for daunorubicin content. Standard curves were prepared in stock rat or rabbit plasma to determine the concentration of daunorubicin for the samples.

2.3.4. HPLC Method for Daunorubicin

HPLC analysis of daunorubicin was done using a Waters Alliance 2695 HPLC with a Waters 2998 photodiode array detector (PDA), and a Waters 2475 fluorescence detector (FLD). The separations unit was equipped with a Waters NovaPak C18 (4 µm, 150 x 3.9 mm) column. Daunorubicin was detected by PDA at a wavelength of 485 nm, and was detected by FLD at excitation of 350 nm and emission at 533 nm. The mobile phases consisted of the following: MP A = methanol; MP B = 10 mM phosphate buffer, pH 2; MP C = acetonitrile. The run consisted of a 12-minute gradient with a flow rate of 1.0 mL/minute. The gradient is shown in Table **1**.

2.3.5. Pharmacokinetics and Statistical Analysis

Pharmacokinetic parameters for the noncompartmental analysis of rat and rabbit studies were determined using Phoenix WinNonlin version 6.3.

2.4. IT-143 *In vitro*

2.4.1. Cell Lines

HCT116 colorectal carcinoma (no. CCL-247), HT1080 fibrosarcoma (no. CCL-121), MNNG cells (no. CRL-1547), MG-63 osteosarcoma (no. CRL-1427), A549 lung carcinoma (no. CCL-185), and A375 malignant melanoma (CRL-1619) were all purchased from ATCC. McCoy's Minimum

Table 1. Mobile Phase Gradient for HPLC Analysis of Daunorubicin.

Time	% A	% B	% C	Curve
0	10	70	20	6
1.5	10	70	20	6
8	10	40	50	6
10	10	40	50	6
11	10	70	20	6
12	10	70	20	6

Essential Medium, MEM with Earle's Balanced Salt Solution (EBSS), F-12K media, Dulbecco's Modified Eagle's Medium (DMEM) media, Penicillin/Streptomycin, Non-Essential Amino Acid, (NEAA) Solution, 100X, Phosphate Buffered Saline were purchased from Thermo Fisher. Fetal Bovine Serum was purchased from Hyclone. Trypsin was purchased from Corning. All cell lines were cultured *in vitro* with 1% Penicillin/ Streptomycin in a humidified atmosphere at 37°C with 5% CO_2. HCT116 were cultured in McCoy's media with 10% FBS. HT1080, MNNG, and MG-63 were cultured with MEM media including 1X NEAA and 1% sodium pyruvate. A375 were cultured with DMEM. A549 were cultured with F-12K media.

2.4.2. In vitro Cytotoxicity

Five types of cell lines were seeded in 96-well white walled plates. Cells were plated so that 96 hr. after seeding, untreated control wells would not exceed 90% confluence. HCT116 were seeded at 2.0 x 10^3 cells/well, A549 at 950 cells/well, A375 at 1.1 x 10^3 cells/well, MG-63 at 2x10^3 cells/well, and HT1080 at 7.5 x 10^2 cells/well. All plates were also dosed with Cisplatin (ACROS organics) as an internal positive control and cells treated with media alone as a negative control. Empty unseeded wells were used as a background control for cytotoxicity assay reagents. Four plates per cell line were plated in order to duplicate dilutions with Cell Titer Blue (Promega) an intracellular adenosine triphosphate assay and Cell Titer Glo (Promega) a resazurin reduction assay. Plates were seeded in 50 µL of designated cell media and dosed with 50 µL of treatment diluted in media in an escalating dilution scheme 24 hr. after seeding for a total well volume of 100 µL. Plates were incubated for 72 hr. with treatment dilutions and metabolic assays applied according to manufactures' protocols and read on Perkin Elmer Enspire Multimode plate reader.

2.5. IT-143 *In vivo*

2.5.1. Animals

Mice were 6-week old female athymic nudes obtained from Charles River Laboratories (MA, USA) and maintained in pathogen-limited conditions. Mice were given food and water *ad libitum*. Efficacy dose response was achieved by adjusting the volume of treatment injection calculated based on animal's weight. Mice were humanely euthanized if tumors ulcerated, impeded mobility, or affected general health. This study was conducted under IACUC Approved Animal Use Protocol #0624R.

2.5.2. HCT116 Xenograft Model

Cells were thawed from liquid nitrogen storage reconstituted in warmed media. As cells reached 80% confluency they were split into T-150 flasks until the required number of cells was ready for harvest. On the day of inoculation, HCT116 cells at passage 16 were trypsinized, counted, resuspended in PBS, and kept on ice. 45 female, athymic nude mice were inoculated with 1 million cells in a 100 µL bolus injection. Cells were implanted subcutaneously on the right flank of each mouse.

2.5.3. HT1080 Xenograft Model

On the day of inoculation, HT1080 cells at passage 8 were trypsinized, counted, resuspended in PBS, and kept on ice. 50 female, athymic nude mice were inoculated with 5 x 10^5 cells in a 100 µL bolus injection. Cells were implanted subcutaneously on the right flank of each mouse.

2.5.4. MNNG Xenograft Model

On the day of inoculation MNNG cells at passage 7 were trypsinized, counted, resuspended in basal MEM media, and kept on ice. 70 female, athymic nude mice were inoculated with 2 million cells suspended in a 100 µl injection of media/ matrigel 50/50 (v/v) injection. Cells were implanted subcutaneously on the right hindquarter of each mouse.

3. RESULTS

3.1. IT-143 – Micelle Encapsulation of Daunorubicin

IT-143 is a lyophilized formulation of daunorubicin encapsulated in a polymer micelle (ITP-102 (Scheme **1**)). The specialized formulation characteristics of IT-143 improve drug solubility, pharmacokinetics, and efficacy of daunorubicin without modifying the drug structure. The PEGylated outer

structure allows for steric shielding of the nanoparticle while the inner core contains encapsulated daunorubicin (Fig. **1**). This "stealth" outer layer prevents nanoparticle aggregation and absorption by opsonin proteins and phagocytic cells that would sequester non-protected nanoparticles and free daunorubicin to the liver and spleen [24-26]. Further iron crosslinking of the core stabilizes the micelle. When below the critical micelle concentration (CMC) the nanoparticles do not quickly degrade nor aggregate. This stabilization suitably prolongs plasma half-life and increases nanoparticle drug retention. Paired with EPR exploitation and MPS evasion the proposed acidic tumor conditions, in contrast to the surrounding normal tissue, provides favorable conditions for the degradation of the drug delivering nanoparticle [27]. The physical characteristics of IT-143 result an average particle diameter of 58 nm allowing it to utilize tumor specific characteristics for drug delivery and tissue targeting.

Formulation control was prepared by mimicking the encapsulation and subsequent micelle stabilization process described above, but without daunorubicin. Formulation control is comprised of ITP-102, iron, and trehalose and is utilized as a control for *in vivo* experiments.

3.2. IT-143 Formulation Physiochemical Characterization

The formulation of IT-143 resulted in an 82% efficient process, and the total yield of the formulation was 88%. Daunorubicin weight loading for IT-143 was 3.8% of the total formulation weight. For example, 100 mg of IT-143 contains 3.8 mg of daunorubicin. The average particle diameter for IT-143 was 58 nm. Encapsulation of daunorubicin and iron-mediated micelle stabilization of the formulation was demonstrated by dialysis of IT-143 reconstituted above (20 mg/mL) and below (0.2 mg/mL) the CMC compared to unstabilized formulation diluted below the CMC in phosphate buffer (10 mM, pH 7.4). Dialysis of IT-143 reconstituted above the CMC resulted in 95% retention of daunorubicin inside the dialysis bag. Dialysis of IT-143 when diluted below the CMC resulted in 61% retention of daunorubicin, while dialysis of the uncrosslinked formulation below the CMC resulted in 10% retention of daunorubicin. pH-dependent release of daunorubicin from IT-143

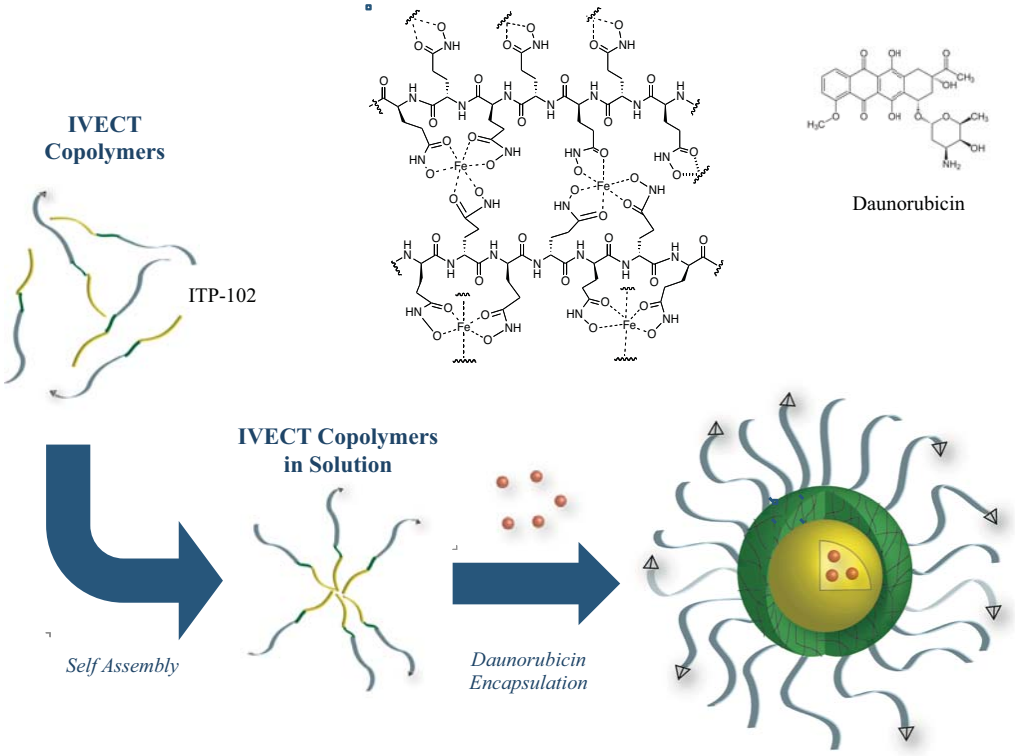

Fig. (1). Schematic illustration depicting the IT-143 formulation process. Inset image shows iron ligation with hydroxamic acid moieties on the polymer chains.

was determined by dialysis of the formulation below the CMC in phosphate buffer at pH 3, 4, 5, 6, 7, 7.4, and 8 (Fig. **2**).

3.3. *In vitro* Characterization

IT-143 and free daunorubicin were screened in 5 human cancer cell lines to compare the half maximal inhibitory concentrations *in vitro*.

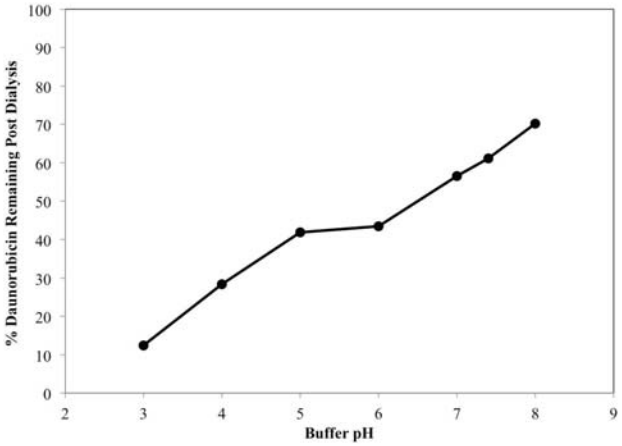

Fig. (2). Results of IT-143 dialysis experiment demonstrating pH dependent release. Percent remaining is calculated as the percentage of daunorubicin remaining in the dialysis bag after 6 hours.

3.3.1. IC50

Five cell lines were seeded in individual 96-well plates and treated with a range of IT-143 or daunorubicin concentrations. At 72 hours, cell numbers in each well were quantitated with a plate reader using cell-titer glo or cell-titer blue assays. The concentration that inhibited cell growth by 50% was determined. Daunorubicin free drug had an IC_{50} ranging between 67-114 nM in the cell lines compared to 60-110 nM for IT-143 (Table **2**).

3.4. *In vivo* Characterization

All dosing of IT-143 is represented herein as the dose equivalent of daunorubicin (e.g. 10 mg/kg IT-143 described below represents 263.2 mg/kg of total IT-143 formulation which is the equivalent of 10 mg/kg total daunorubicin.) We characterized the pharmacokinetics (PK), the maximum tolerated dose (MTD) and the anti-tumor efficacy of IT-143 *in vivo* and compared the results to free daunorubicin. Notably, for the MTD and anti-tumor efficacy studies, IT-143 and daunorubicin were administered intravenously via the lateral tail vein. In the clinic, the protocol for daunorubicin injection is a rapidly flowing intravenous infusion. Extravasation results in severe local tissue necrosis. In our studies some animals in the daunorubicin groups did suffer from some tail tissue necrosis. However, no mice in the IT-143 administered groups were fated due to tail tissue necrosis.

3.4.1. Rat Plasma Pharmacokinetics

Plasma pharmacokinetics of daunorubicin from intravenous administration of the free drug at 10 mg/kg was compared to daunorubicin from IT-143 at 10 and 20 mg/kg equivalent using a cannulated rat model (Fig. **3a**). Test article administration was by fast bolus to the jugular vein catheter followed by blood collection at time points of 1 minute, 5 minutes, 15 minutes, 1 hour, 4 hours, 24 hours, and 48 hours. Daunorubicin from IT-143 at 10 and 20 mg/kg was detectable in the plasma at concentrations above 1 µg/mL to the 48-hour time point, whereas daunorubicin from free drug administration at 10 mg/kg dropped below 1 µg/mL at the 5-minute time point and was below limit of detection at the 48-hour time point. The maximum concentration (C_{max}) of daunorubicin in the plasma from IT-143 administration at 10 and 20 mg/kg was 166.3 and 323.8 µg/mL compared to 3.3 µg/mL from free drug administration. The area under the time versus concentration curve ($AUC_{0\text{-}inf}$) from

Table 2. Summary of IC_{50} values for IT-143 versus daunorubicin in a panel of human cancer cell lines.

	HT-1080	MG-63	HCT116	A549	A375
IT-143	50 nM	139 nM	79 nM	110 nM	60 nM
Daunorubicin	50 nM	206 nM	88 nM	115 nM	67 nM

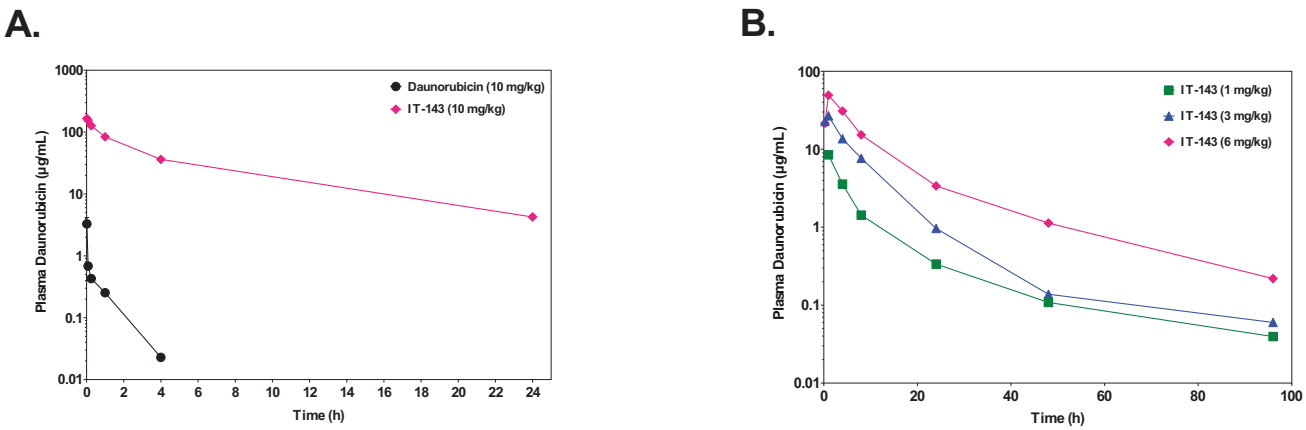

C.

	AUC (h * µg/mL)	C_{Max} (µg/mL)	T_{Max} (h)	Term. $T_{1/2}$ (h)
Daunorubicin (10 mg/kg)	1.44	3.29	0.0167	7.24
IT-143 (10 mg/kg)	783.54	166.28	0.0167	8.03

D.

	AUC (h * µg/mL)	C_{Max} (µg/mL)	T_{Max} (h)	Term. $T_{1/2}$ (h)
IT-143 (1 mg/kg)	62.39	8.48	1	24.33
IT-143 (3 mg/kg)	215.70	26.86	1	10.83
IT-143 (6 mg/kg)	486.92	49.40	1	18.51

Fig. (3). Pharmacokinetic curves of IT-143 and free daunorubicin in (a) rats and (b) rabbits.

IT-143 administration at 10 and 20 mg/kg was 783.5 and 1480.4 h*µg/mL compared to 1.4 h*µg/mL from the free drug at 10 mg/kg.

3.4.2. Rabbit Plasma Pharmacokinetics

Plasma pharmacokinetics of daunorubicin from intravenous administration of the free drug at 3 mg/kg was compared to daunorubicin from IT-143 at 1, 3, and 6 mg/kg equivalent using a cannulated rabbit model (Fig. **3b**). Test articles were administered via 30-minute infusion to the jugular vein catheter, and blood was collected at time points of 1 hour, 4 hours, 8 hours, 24 hours, 48 hours, and 96 hours. Animals treated with 3 and 6 mg/kg IT-143 included an additional blood sampling 15 minutes post infusion. Treatment with the 3 mg/kg dose of the free drug yielded only one plasma sample with daunorubicin above limit of quantitation at the 1-hour time point resulting in a concentration of 0.1 µg/mL. Treatment with 1, 3, and 6 mg/kg daunorubicin from IT-143 resulted in C_{max} concentrations of 8.5, 22.7, and 49.4 µg/mL, respectively. The $AUC_{0\text{-}inf}$ values for the 1, 3, and 6 mg/kg doses were 62.4, 215.7, and 486.9 h*µg/mL, respectively.

3.4.3. Maximum Tolerated Dose

IT-143 as a stably encapsulated crosslinked nanoparticle of daunorubicin allows increased dosing of the drug with decreased toxicities. Dosing in mice reached two and a third times that of the free daunorubicin maximum tolerated dose (MTD) before observed toxicities were reported. Gross toxicities observed at doses over the MTD include ascites, above normal weight gain from the edema, and lethargy. Weight gain was recorded for all groups comparable to control.

MTD studies were run in CD-1 immunocompetent mice and in immunocompromised athymic nude mice. The CD-1 mice 3 groups were dosed at 15, 20, and 25 mg/kg to assess a range of toxicities once weekly for 3 weeks (qwx3). On D13, the 25 mg/kg IT-143 group saw an average weight loss of 9%, but recovery weight gain was seen by D18. The IT-143 20 mg/kg and 15 mg/kg groups saw no weight effect. The maximum weight loss of an individual animal was 17.6%, recorded in the 25 mg/kg IT-143 group on D13. The maximum weight gain of an individual animal was 23.4% and 10.5% on D20, recorded in the 20 mg/kg IT-143. An individual animal weight gain of 10.3% was recorded in the 15 mg/kg IT-143 group on D20. No other animals changed more than 10% of weight from D0 weight. Two animals were found dead on D20 in the 25 mg/kg IT-143 group. Gross observations recorded fluid-filled abdomen and necropsies were carried out on the remaining animals. Results noted an enlarged abdomen with significantly decreased body fat, friable intestines,

discolored liver, and discolored kidneys. The 20 mg/kg IT-143 group demonstrated fluid filled abdomens with the decreased body fat and abnormally enlarged multi-lobed, clear gelatinous pancreases. The maximum tolerated dose was determined to be between 20 mg/kg and 15 mg/kg for IT-143.

As weight gain or weight loss was not a robust marker for daunorubicin toxicity, gross observations and necropsies were performed to determine the MTD. Athymic nude mice were grouped into 4 and treated qwx3 at 17.5 or 20 mg/kg with IT-143 and compared to 7.5 or 10 mg/kg free daunorubicin treated groups. On D14 both the 20 mg/kg IT-143 and the 10 mg/kg free daunorubicin groups were euthanized and necropsied due to poor health and edema. On D18 and D20 the 17.5 mg/kg IT-143 group and the 7.5 mg/kg daunorubicin groups were euthanized and necropsied respectively. The dose limiting toxicities for 20 mg/kg IT-143 and 10 mg/kg free daunorubicin were comparable with fluid filled abdomens, reduced body fat, small spleens, occasional liver discoloration, and abnormal pancreas. These side effects were only mildly noted in one animal of both the 17.5 mg/kg IT-143 group and the 7.5 mg/kg free daunorubicin group. The maximum tolerated dose of IT-143 on a qwx3 dose schedule was therefore determined to be 17.5 mg/kg and 7.5 mg/kg for free daunorubicin.

3.4.4. Tumor Efficacy

A decrease in relative tumor volume over the course of the treatment was achieved higher than that of free drug administration in three tumor xenograft efficacies (Fig. **4**). Dosing of IT-143 with 7.5 mg/kg of equivalent daunorubicin compared to free daunorubicin demonstrated equal or less change over time in relative tumor volume in two out of the three models. Free daunorubicin treated at the MTD for this dosing schedule was not effective above control in two out of the three models. Free daunorubicin demonstrated minimal efficacy in the MNNG model. The MNNG model was noted to invade muscle tissue, which compounded the ability to accurately measure tumor volume externally with calipers.

HCT116 tumors were established on the right flank of nude athymic mice. The average tumor volume on D0 was 177 mm^3. Mice were randomized into five groups of eight. Tumor volume deviation for each group was less than 10%. The average weight of animals on D0 was 23.2 g. Formulation Control, daunorubicin, and IT-143 were administered intravenously via the lateral tail vein on a dosing schedule of qwx3. Tumor volume measurements and animal weights were recorded three times a week. Throughout the study no group had weight change greater than 3% from starting weight (Fig. **4d**). Relative tumor volume inhibition for both IT-143 treatment groups showed efficacy over free daunorubicin and control. In this model the relative tumor volume fold change for 7.5 mg/kg free daunorubicin treatment was 10-fold compared to a 4.7-fold change for the 7.5 mg/kg IT-143 and a 3.4-fold change for the 17.5 mg/kg IT-143 groups. (Fig. **4a**) Tumor growth inhibition (%TGI) for IT-143 was 41% for the 7.5 mg/kg group and 88% for the 17.5 mg/kg group (Table **3**).

HT-1080 inoculated mice were randomized into 5 groups of 10. Tumor volume deviation for each group was less than 13%. The average tumor volume nine days after inoculation on D0 was 111 mm^3. The average weight of animals on D0 was 23.2 g. Throughout the study no group recorded weight change greater then 5% (Fig. **4e**). The relative tumor volume fold change for control group was 19.9 from D0 to D19 (Fig. **4b**). The free daunorubicin treatment group saw a 14.4-fold change compared to an 11.4-fold change observed in the IT-143 7.5 mg/kg equivalent dose group. The 17.5 mg/kg IT-143 group had only a 1.59-fold change from D0 to D19. %TGI for free daunorubicin was 28% compared to 43% in the 7.5 mg/kg and 92% in the 17.5 mg/kg group (Table **3**). Tumor volume deviation for each group was less than 13%.

MNNG-HOS inoculated mice were randomized into 5 groups of 12. Tumor volume deviation for each group on study D0 for each group was less than 13%. The average tumor volume 15 days after inoculation on D0 was 114 mm^3. The average weight of animals on D0 was 22.8 g. The free daunorubicin group experienced an increase in weight towards the end of the study due to ascites (Fig. **4f**). No other groups in the study experienced a weight change greater the 5%. All treatment groups demonstrated relative tumor volume efficacy compared to control group (Fig. **4c**). The relative tumor fold-change for control group was 7.8 from D0 to study end on D19. Free daunorubicin treatment group had a 4.4-fold growth rate

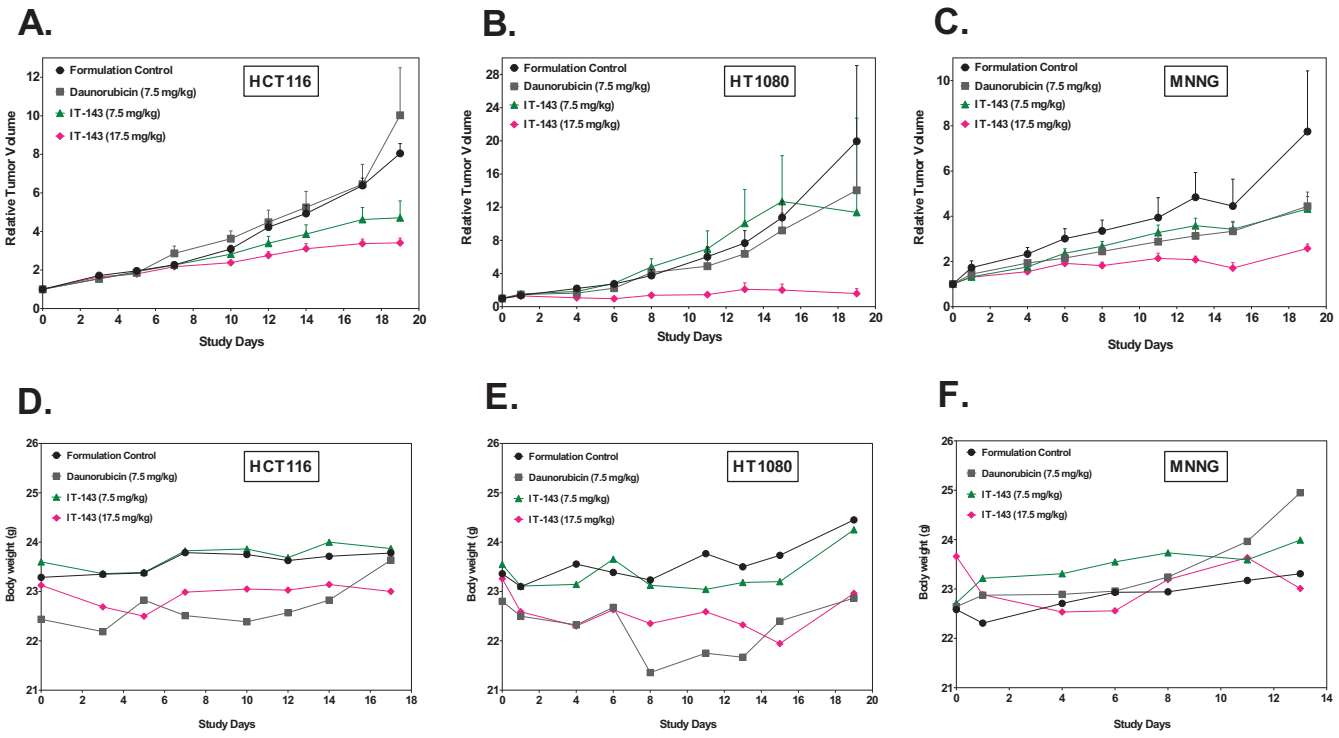

G.

	Dose IT-143 mg/kg/dose	Dose daunorubicin mg/kg/dose
Formulation Control	N/A	N/A
Daunorubicin (7.5 mg/kg)	N/A	7.5
IT-143 (7.5 mg/kg)	202.70	7.5
IT-143 (17.5 mg/kg)	472.97	17.5

Fig. (4). Xenograft efficacy models following dosing of IT-143 and daunorubicin are depicted. Panels A. through C. represent tumor growth curves for HCT116, HT1080, and MNNG models, respectively. Panels D. through E. represent group average body weight throughout the experiment. Panel G. describes dose levels for each group.

Table 3. Summary of tumor growth data for xenograft efficacy experiments comparing IT-143 to free daunorubicin.

Treatment	HCT116		HT1080		MNNG	
	% TGI	Fold Change (D0 to D19)	% TGI	Fold Change (D0 to D19)	% TGI	Fold Change (D0 to D19)
Formulation Control	-	8.1	-	19.9	-	7.8
Daunorubicin (7.5 mg/kg)	0%	10	28%	14.4	43%	4.4
IT-143 (7.5 mg/kg)	41%	4.7	43%	11.4	44%	4.3
IT-143 (17.5 mg/kg)	88%	3.4	92%	1.59	67%	2.6

compared to a 4.3-fold change in the IT-143 7.5 mg/kg group. The 17.5 mg/kg IT-143 recorded a 2.6-fold change from D0 to D19. %TGI was 43% for free daunorubicin compared to 44% for IT-143 and 67% for the 17.5 mg/kg IT-143 group (Table **3**).

4. DISCUSSION

We have shown herein that IT-143 significantly improves the pharmacokinetic parameters, efficacy, and toxicity of daunorubicin. The Cmax of daunorubicin was increased in excess of 50-fold

for IT-143 using equivalent doses in rat models. The plasma exposure was increased several hundred-fold in both rats and rabbits leading to a widened therapeutic window for daunorubicin, both in terms of increased efficacy at equivalent doses and in terms of the maximum tolerated dose.

Based upon the significant changes in the pharmacokinetic parameters, we infer that the iron-mediated stability sequesters the daunorubicin in the core of intact micelles in the bloodstream. The increased circulation time is not seen with uncrosslinked micelles and the PK of uncrosslinked micelles is comparable to the PK results of free drug (data not shown). The stability from the crosslinking not only improves the pharmacokinetics and circulation time, but also leads to increased accumulation at the tumor site from the EPR effect. The EPR effect is based on Maeda's theory that vessels in tumors are defective and therefore the improved circulation time allow more micelles to escape and accumulate in the tumor milieu. Biodistribution studies with our drug delivery platform demonstrate improved accumulation in healthy tissue too, but we suggest the pH change in the tumor environment results in targeted drug delivery, reduced non-targeted toxicity, and improved efficacy.

The polymeric make-up of IT-143 promises escape from immune responses seen with PEGylated liposome nanoparticles [28]. Additionally, the iron crosslinking of IT-143 was not notably observed to potentiate the gross cardiotoxic effects of daunorubicin. However, additional studies are required to further investigate these observations, specifically with regard to the combination of iron with anthracyclines [1]. Measurements of germane cardiotoxicity parameters will be needed to determine whether IT-143 is able to decrease the daunorubicin-related toxicities. The known difficulties of conducting cardiotoxicity studies in rabbit models, [29, 30] promotes the use of a more robust model such as dogs. These studies will be required to ultimately determine the potential benefit of IT-143 over free daunorubicin for long-term cardiotoxicity protection.

Although the micelle encapsulation of daunorubicin has been utilized here to elicit tumor response and show potential for increased patient survival, there are known inherit limitations to nanoparticle delivery. Heterogeneity of EPR in different tumor types and variable activity of the MPS can influence targeting of tumor tissue. The need for future studies in different tumor models such as orthotopic models or primary explants could aid in predictive patient tumor response. Contrast agents with nanoparticles and magnetic resonance imaging (MRI) could provide opportunity to measure enhanced permeability of tumor tissue with drug delivery.

Research reported in this publication was supported by the National Cancer Institute of the National Institutes of Health under Award Number U43CA179468. The content is solely the responsibility of the authors and does not necessarily represent the official views of the National Institutes of Health.

CONFLICT OF INTEREST

The author(s) confirm that this article content has no conflict of interest.

ACKNOWLEDGEMENTS

Research reported in this publication was supported by National Cancer Institute of the National Institutes of Health under award number U43CA179468. The content is solely the responsibility of the authors and does not necessarily represent the official views of the National Institutes of Health.

The authors would like to thank Matt Davis for his valuable contribution with the data presentation in this paper.

REFERENCES

[1] Minotti G, Menna P, Salvatorelli E, Cairo G, Gianni L. Anthracyclines: molecular advances and pharmacologic developments in antitumor activity and cardiotoxicity. Pharmacol Rev 2004; 56: 185-229.

[2] Rahman AM, Yusuf SW, Ewer MS. Anthracycline-induced cardiotoxicity and the cardiac-sparing effect of liposomal formulation. Int J Nanomedicine 2007; 2(4): 567-83.

[3] Lencova-Popelova O, Jirkovsky E, Mazurova Y, *et al.* Molecular remodeling of left and right ventricular myocardium in chronic anthracycline cardiotoxicity and post-treatment follow up. PLoS One 2014; 9(5): e96055.

[4] Oliveira GH, Al-Kindi SG, Caimi PF, Lazarus HM. Maximizing anthracycline tolerability in hematologic malignancies: Treat to each heart's content. Blood Rev 2015 [Epub ahead of print].

[5] Nitiss JL. Targeting DNA topoisomerase II in cancer chemotherapy. Nat Rev Cancer 2009; 9(5): 338-50.
[6] Pharmaceuticals G. DAUNOrubicin HCl For Injections, USP Package Insert 1999.
[7] Gallois L, Fiallo M, Garnier-Suillerot A. Comparison of the interaction of doxorubicin, daunorubicin, idarubicin and idarubicinol with large unilamellar vesicles. Circular dichroism study. Biochim Biophys Acta 1998; 1370(1): 31-40.
[8] Ma P, Mumper RJ. Anthracycline Nano-Delivery Systems to Overcome Multiple Drug Resistance: A comprehensive review. Nano Today 2013; 8(3): 313-31.
[9] Chen Z, Chen HC, Montell C. TRP and rhodopsin transport depends on Dual XPORT ER chaperones encoded by an operon. Cell reports 2015.
[10] Song H, Zhang J, Han Z, *et al.* Pharmacokinetic and cytotoxic studies of pegylated liposomal daunorubicin. Cancer Chemother Pharmacol 2005; 57: 591-8.
[11] O'brien MER. Reduced cardiotoxicity and comparable efficacy in a phase III trial of pegylated liposomal doxorubicin HCl (CAELYXTM/Doxil") versus conventional doxorubicin for first-line treatment of metastatic breast cancer. Ann Oncol 2004; 15(3): 440-9.
[12] Lorusso V, Manzione L, Silvestris N. Role of liposomal anthracyclines in breast cancer. Annal Oncol 2007; 18 Suppl 6: vi70-3.
[13] Yokoyama M, Fukushima S, Uehara R, *et al.* Characterization of physical entrapment and chemical conjugation of adriamycin in polymeric micelles and their design for *in vivo* delivery to a solid tumor. J Control Rel 1998; 50(1): 79-92.
[14] Talelli M, Barz M, Rijcken CJ, *et al.* Core-crosslinked polymeric micelles: Principles, preparation, biomedical applications and clinical translation. Nano Today 2015; 10(1): 93-117.
[15] Bouzin C, Feron O. Targeting tumor stroma and exploiting mature tumor vasculature to improve anticancer drug delivery. Drug Resist Updates 2007; 10(3): 109-20.
[16] Au JL, Jang SH, Zheng J, *et al.* Determinants of drug delivery and transport to solid tumors. J Control Rel 2001; 74: 31-46.
[17] Prabhakar U, Maeda H, Jain RK, *et al.* Challenges and key considerations of the enhanced permeability and retention effect for nanomedicine drug delivery in oncology. Cancer Res 2013; 73(8): 2412-7.
[18] Hiroshi Maeda TSTK. The enhanced permeability and retention (EPR) effect in tumor vasculature: The key role of tumor-selective macromolecular drug targeting. Advan Enzyme Regul 2001; 41: 189-207.
[19] Maeda H, Wu J, Sawa T, Matsumura Y, Hori K. Tumor vascular permeability and the EPR effect in macromolecular therapeutics: A review. J Control Rel 2000; 65: 271-84.
[20] Arap W, Pasqualini R, Ruoslahti E. Cancer treatment by targeted drug delivery to tumor vasculature in a mouse model. Science 1998; 279: 377-80.
[21] Greish K. Enhanced permeability and retention of macromolecular drugs in solid tumors: A royal gate for targeted anticancer nanomedicines. J Drug Target 2007; 15(7-8): 457-64.
[22] Maeda H. The enhanced permeability and retention (EPR) effect in tumor vasculature: The key role of tumor-selective macromolecular drug targeting. Adv Enzyme Regul 2001; 41: 189-207.
[23] Maeda H. Vascular permeability in cancer and infection as related to macromolecular drug delivery, with emphasis on the EPR effect for tumor-selective drug targeting. Proceedings of the Japan Academy, Series B. 2012; 88(3): 53-71.
[24] Jokerst JV, Lobovkina T, Zare RN, Gambhir SS. Nanoparticle PEGylation for imaging and therapy. Nanomedicine (Lond) 2011; 6(4): 715-28.
[25] Owens DE 3rd, Peppas NA. Opsonization, biodistribution, and pharmacokinetics of polymeric nanoparticles. Int J Pharm 2006; 307(1): 93-102.
[26] Romberg B, Hennink WE, Storm G. Sheddable coatings for long-circulating nanoparticles. Pharm Res 2008; 25(1): 55-71.
[27] Ojugo AS, Mcsheehy PM, Mcintyre DJ, *et al.* Measurement of the extracellular pH of solid tumours in mice by magnetic resonance spectroscopy: A comparison of exogenous (19)F and (31)P probes. NMR Biomed 1999; 12(8): 495-504.
[28] Semple SC, Harasym TO, Clow KA, *et al.* Immunogenicity and rapid blood clearance of liposomes containing polyethylene glycol-lipid conjugates and nucleic Acid. J Pharmacol Exp Ther 2005; 312(3): 1020-6.
[29] Calasans-Maia MD, Monteiro ML, Ascoli FO, Granjeiro JM. The rabbit as an animal model for experimental surgery. Acta Cir Bras 2009; 24(4): 325-8.
[30] Mapara M, Thomas BS, Bhat KM. Rabbit as an animal model for experimental research. Dent Res J 2012; 9(1): 111-8.

Received: January 07, 2016 Revised: February 25, 2016 Accepted: March 07, 2016